A DNA methylation fingerprint of 1,628 human samples

Agustin F Fernandez, Yassen Assenov, Jose Martin-Subero, et al.

Genome Res. published online May 25, 2011
Access the most recent version at doi:10.1101/gr.119867.110

A DNA Methylation Fingerprint of 1,628 Human Samples

Agustin F. Fernandez, Yassen Assenov, Jose Ignacio Martin-Subero, Balazs Balint, Reiner Siebert, Hiroaki Taniguchi, Hiroyuki Yamamoto, Manuel Hidalgo, Aik-Choon Tan, Oliver Galm, Isidre Ferrer, Montse Sanchez-Cespedes, Alberto Villanueva, Javier Carmona, Jose V. Sanchez-Mut, Maria Berdasco, Victor Moreno, Gabriel Capella, David Monk, Esteban Ballestar, Santiago Ropero, Ramon Martinez, Marta Sanchez-Carbayo, Felipe Prosper, Xabier Agirre, Mario F. Fraga, Osvaldo Graña, Luis Perez-Jurado, Jaume Mora, Susana Puig, Jaime Prat, Lina Badimon, Annibale A. Puca, Stephen J. Meltzer, Thomas Lengauer, John Bridgewater, Christoph Bock & Manel Esteller

Cancer Epigenetics and Biology Program (PEBC), Bellvitge Biomedical Research Institute (IDIBELL), L'Hospitalet, Barcelona, Catalonia, Spain (AFF, JIMS, BB, HT, MSC, JC, JVSM, MB, DM, EB, ME)
Max-Planck-Institut for Informatics, Saarbrücken, Germany (YA, TL, CB)
Institute of Human Genetics, Christian-Albrechts-University Kiel and University Hospital Schleswig-Holstein, Campus Kiel, Kiel, Germany (IMS, RS)
The Sidney Kimmel Comprehensive Cancer Center at Johns Hopkins University School of Medicine, Baltimore, MD, USA (MH, SJM)
Division of Medical Oncology, University of Colorado School of Medicine, Aurora, CO, USA (ACT)
First Department of Internal Medicine, Sapporo Medical University School of Medicine,Sapporo,Japan (HT)
Medizinische Klinik IV, Universitaetsklinikum Aachen, RWTH Aachen, Germany. (OG)
Institut de Neuropatologia, IDIBELL-Hospital Universitari de Bellvitge, Universitat de Barcelona, Hospitalet de LLobregat, CIBERNED, L'Hospitalet, Barcelona, Catalonia, Spain (IF)
Translational Research Laboratory, Catalan Institute of Oncology, IDIBELL, L'Hospitalet, Barcelona, Catalonia, Spain (AV, GC)
Biomarkers and Susceptibility Unit, Cancer Prevention and Control Program, Catalan Institute of Oncology, IDIBELL and University of Barcelona, L'Hospitalet, Barcelona, Catalonia, Spain (VM)
Biochemistry and Molecular Biology Department, Alcala University, Madrid, Spain (SR)
Department of Neurosurgery, University of Goettingen, Goettingen WT-084071, Germany (RM)
Spanish National Cancer Research Centre (CNIO), Madrid, Spain (MSC, MH, OG)
Division of Oncology, Center for Applied Medical Research, University of Navarra, Avda. Pio XII, Pamplona, Spain (FP, XA)
Instituto Universitario de Oncología del Principado de Asturias (IUOPA), Universidad de Oviedo, Oviedo, Spain (AFF)
Department of Immunology and Oncology, National Center for Biotechnology, CNB-CSIC, Cantoblanco, Madrid E-28049, Spain (MFF)
Departament de Ciències Experimentals i de la Salut, Universitat Pompeu Fabra, E-08003 Barcelona, Spain; Centro de Investigación Biomédica en Red de Enfermedades Raras (CIBERER), E-08003 Barcelona, Catalonia, Spain (LPJ)
Department of Pediatric Oncology, Hospital Sant Joan de Déu, Barcelona, Catalonia, Spain (JM)
Melanoma Unit, Dermatology Department, Hospital Clinic, Barcelona, Catalonia, Spain (SP)
Hospital de la Santa Creu i Sant Pau, Autonomous University of Barcelona, Barcelona, Spain (JP)
Cardiovascular Research Center, CSIC-ICCC, Hospital Sant Pau, Barcelona, Catalonia, Spain (LB)
Unit of Genetics and Cardiovascular Research Institute, Istituto Ricovero Cura Carattere Scientifico Multimedica, Sesto S. Giovanni, Italy (AAP)
Division of Gastroenterology, Department of Medicine, the Johns Hopkins University School of Medicine, Baltimore, Maryland, USA (SJM)
University College London Cancer Institute, London WC1E 6DD, UK (JB)
Broad Institute, Cambridge, MA, USA (CB)
Department of Stem Cell and Regenerative Biology, Harvard University, Cambridge, MA, USA (CB)
Department of Physiological Sciences II, School of Medicine, University of Barcelona, Barcelona, Catalonia, Spain (ME)
Institucio Catalana de Recerca i Estudis Avançats (ICREA), Barcelona, Catalonia, Spain (ME)

Correspondence should be addressed to ME (mesteller@idibell.cat)

Abstract

DNA methylation is the best characterized of the different layers that make up the epigenetic setting. Most of the studies characterizing DNA methylation patterns have been restricted to particular genomic loci in a limited number of human samples and pathological conditions. The recently arrived single-base-resolution technologies for DNA methylation are extremely helpful tools, but are not yet applicable and affordable for studying large groups of subjects. Herein, we present a compromise between an extremely comprehensive study of a human sample population with an intermediate level of resolution of CpGs at the genomic level. We obtained a DNA methylation fingerprint of 1,628 human samples where we interrogated 1,505 CpG sites. The DNA methylation patterns revealed show this epigenetic mark to be critical in tissue-type definition and stemness, particularly around transcription start sites that are not within a CpG island. For disease, the generated DNA methylation fingerprints show that, during tumorigenesis, human cancer cells underwent a progressive gain of promoter CpG island hypermethylation and a loss of CpG methylation in non-CpG island promoters. Although transformed cells are those where DNA methylation disruption is more obvious, we observed that other common human diseases, such as neurological and autoimmune disorders, had their own distinct DNA methylation profiles. Most importantly, we provide proof of principle that the obtained DNA methylation fingerprints might be useful for translational purposes by showing that are able to identify the tumor type origin of Cancers of Unknown Primary (CUPs). Thus, the DNA methylation patterns identified across the largest spectrum of samples, tissues and diseases reported to date constitute a baseline for developing higher-resolution DNA methylation maps, and provide important clues concerning the contribution of CpG methylation to tissue identity and its changes in the most prevalent human diseases.

The microarray data from this study have been submitted to the NCBI Gene Expression Omnibus (http://www.ncbi.nlm.nih.gov/geo) under accession number GSE28094.

INTRODUCTION

Epigenetics encompasses a large number of mechanisms underlying embryonic development, differentiation and cell identity, including DNA methylation and histone modifications (Bernstein et al. 2007; Hemberger et al., 2009). The existence of distinct epigenomes might explain why the same genotypes generate different phenotypes, such as those seen in Agouti mice (Michaud et al. 1994), cloned animals (Humpherys et al. 2001), and monozygotic twins (Fraga et al. 2005; Kaminsky et al., 2009). Most importantly, epigenetic alterations are increasingly recognized as being involved in human diseases (Das et al. 2009), such as cancer (Jones and Baylin 2007; Esteller 2008) and imprinting (Feinberg 2007), neurological, (Urdinguio et al., 2009), cardiovascular (Gluckman et al., 2009) and autoimmune (Richardson, 2007) disorders, among others. For the first time it is possible to define whole epigenomes, which represent all epigenetic marks in a given cell type, thanks to the development of powerful new genomic technologies (Bernstein et al. 2007; Esteller 2007; Jones and Baylin 2007; Bonetta 2008; Lister and Ecker 2009). Furthermore, coordinated epigenomic projects are starting to be launched (Jones et al., 2008; Abbot 2010).

One of the earliest studied epigenetic marks in eukaryotes is cytosine DNA methylation, which acts as a stably inherited modification affecting gene activity and cellular biology. Determining the complete DNA methylome entails describing all the methylated nucleotides in an organism. The gold standard technique for analyzing the methylation state of individual cytosines is bisulfite sequencing in which unmethylated cytosines are converted to uracils and read as thymines, while methylated cytosines are protected from conversion. Bisulfite sequencing yields precise nucleotide resolution data, but this method has been limited to relatively small genome coverage (Rakyan et al. 2004; Eckhardt et al. 2006; Frigola et al. 2006; Zhang et al., 2009), although it has proved useful for analyzing viral DNA methylomes (Fernandez et al., 2009). Alternative approaches involve the isolation of methylated fractions of the genome by methylation-sensitive restriction (Lippman et al. 2005; Irizarry et al., 2008), or

immunoprecipitation with a methylcytosine (Weber et al. 2005; Keshet et al. 2006; Weber et al., 2007; Down et al., 2008) or methyl-CpG binding domain antibody (Ballestar et al., 2003; Rauch et al., 2009), combined with hybridization to genomic microarrays or ultrasequencing. This is exemplified by the recent DNA methylation analyses of the *Arabidopsis* genome (Zhang et al. 2006; Vaughn et al. 2007; Zilberman et al. 2007), which are further expanded by using sequencing-by-synthesis (MethylC-Seq) technology (Lister et al. 2008) and shotgun bisulfite genomic sequencing (Cokus et al., 2008). In representing mouse pluripotent and differentiated cells, bisulfite sequencing has covered roughly 1 million distinct CpG dinucleotides (4.8% of all CpGs) (Meissner et al., 2008) and two human cell lines (one each from embryonic stem cells and fetal fibroblasts) have been analyzed using MethylC-Seq, including 94% of the cytosines in the genome (Lister et al., 2009). Using whole-genome bisulfite sequencing, the DNA methylome analysis of peripheral blood mononuclear cells from a single-case has also been recently reported (Li et al., 2010).

Only a small number of base-resolution DNA methylomes have been described so far. Nevertheless, even with the enormous advantages that genetic sequencing has over DNA methylation characterization with respect to time and technology, very few full genomes have been reported, either. From the genetic standpoint, this current shortage of information is being tackled through the development of efforts such as the 1,000 Genomes Project (Siva 2008; Kuehn 2008) or by genome-wide association scan (GWAS) studies in which an association with a phenotype or a disease can be established if we limit the number of nucleotides assessed and thus the extent of coverage of the genome (Cantor et al., 2010; Ku et al., 2010). We decided to combine these two approaches —extremely extensive analyses of hundreds of normal and disease-associated cells and tissues with intermediate coverage of CpG dinucleotides— to obtain a DNA methylation fingerprint of 1,628 human samples corresponding to healthy individuals and in those affected by the diseases most commonly associated with death in the western world, such as cancer, neurological disorders and cardiovascular disease.

RESULTS

Description of 1,628 samples and analysis of 1,505 CpG sites

We first studied the genomic DNA from 1,628 human samples corresponding to 424 normal tissues (180 leukocytes, 97 colon mucosa and 227 other normal samples), 1,054 tumorigenic samples (premalignant lesions, primary tumors and metastases) and 150 non-cancerous disorders, such as brain lesions from Alzheimer's disease, dementia with Lewy bodies, aortic atherosclerotic lesions, myopathies and autoimmune disorders. **Supplementary Table 1** shows the complete list of samples studied. The age of donors ranged from six months to 102 years, with an average age of 57 years. 40% (n = 648) were men, 38% (n = 623) were women, the gender of the remaining 22% (n = 357) not being known. 87% (n = 1,421) of the samples were from European volunteers and patients, while 4% (n = 59) and 2% (n = 36) were from Asian and North American populations, respectively; the origin was not known for 7% (n = 112) of cases. Finally, 93% (n = 1,512) of the samples were primary tissues obtained at the time of the clinically indicated procedures, while 7% (n = 116) were obtained from established cell lines. **Supplementary Figure 1** summarizes the described sample distribution. For all these samples we obtained the DNA methylation fingerprints defined by the status of 1,505 CpG sites located from -1,500 bp to +500 bp around the transcription start sites (**Supplementary Figure 2**) of 808 selected genes using the GoldenGate® DNA methylation BeadArray (Illumina, Inc.) assay (Bibikova et al., 2006; Christensen et al., 2009; Byun et al., 2009). The panel of genes includes oncogenes and tumor suppressor genes, imprinted genes, genes involved in various signaling pathways, and those responsible for DNA repair, cell cycle control, metastasis, differentiation and apoptosis (Bibikova et al., 2006; Christensen et al., 2009; Byun et al., 2009). 69% (n = 1,044) of the 1,505 CpG sites studied are located within a canonical CpG island (Takai and Jones, 2002), while 31% (n = 461) are situated outside CpG islands (**Supplementary Figure 2**). All human chromosomes, except the Y-chromosome, are represented among the CpG

sites analyzed (**Supplementary Figure 2**). CpG sites in "CpG island shores", regions of comparatively low CpG density within 2 Kb of CpG islands, are not printed in the array used and their biological relevance has already been extensively studied (Irizarry et al., 2009; Doi et al., 2009). Briefly, in our case, four probes were designed for each CpG site: two allele-specific oligos (ASOs) and two locus-specific oligos (LSOs). Each ASO-LSO oligo pair corresponded to either the methylated or unmethylated state of the CpG site. After bisulfite treatment conversion, the remaining assay steps were identical to those of the GoldenGate® genotyping assay using Illumina-supplied reagents and conditions, and the arrays were imaged using a BeadArray Reader (Illumina Inc.). Each methylation data point was represented by fluorescent signals from the M (methylated) and U (unmethylated) alleles. Before analyzing the CpG methylation data, we excluded possible sources of technical biases that could have influenced the results. Every beta value in the GoldenGate® platform is accompanied by a detection p-value, and we observed that a threshold p-value above 0.01 indicated unreliable beta values (130 CpGs). X-chromosome CpG sites with female-specific DNA methylation (Reik and Lewis, 2005) were also excluded (44 CpGs). Finally, 9 CpG sites that were unmethylated in all normal and disease-associated samples were also excluded. Using these filters, 1,322 CpGs proved to be reliable and were used subsequently in the study. Further technical information is provided in **Supplementary Methods**. The precise DNA methylation status of every CpG dinucleotide analyzed in each of the 1,628 samples studied is freely available by downloading from NCBI Gene Expression Omnibus (http://www.ncbi.nlm.nih.gov/geo) under accession number GSE28094.

DNA methylation fingerprint of human normal tissues

We analyzed first the DNA methylation fingerprints for 424 human normal tissues. Of the 424 normal tissues studied, only 1% (n = 17) of CpGs (corresponding to 14 genes) were methylated in all the samples studied (**Supplementary Table 2**). These exclusively methylated CpG dinucleotides were preferentially located outside CpG islands (82%) (Fisher's exact test, $p=1.97e^{-5}$). Conversely, 37% (n = 488) of the CpGs, corresponding to 359 5'-

ends of genes, were exclusively unmethylated in every normal tissue studied (**Supplementary Table 3**). These always-unmethylated CpG dinucleotides were almost exclusively located within CpG islands (98%) (Fisher's exact test, $p=2.20e^{-85}$) and were associated with housekeeping expression genes (Fisher's exact test, $p=1.13e^{-4}$) (**Supplementary Methods**)*.* Most importantly, significant differential DNA methylation (Kruskal-Wallis rank sum test, $p<2.21e^{-16}$) was encountered between different normal samples of 511 CpG dinucleotides using elastic net classifiers, which enabled their distinction on the basis of tissue type using an unsupervised hierarchical clustering approach (**Figure 1a**). The 511 CpG sites described correspond to 359 genes and, providing further validation to the data, 220 genes (61%) (220) and 137 (38%) were previously identified as genes with tissue-specific DNA methylation using the same 1,505 CpG platform (Byun et al., 2009) or a 27,000 CpG microarray (Nagae et al., 2011), respectively. Illustrative examples of genes found in the three sets, and also confirmed by bisulfite genomic sequencing in another independent study (Eckhardt et al., 2006), include TBX1 (T-Box 1), OSM (Oncostatin M) and GP1BB (Glycoprotein IB Platelet Beta Polypeptide). Examples of tissue-specific CpG methylation further validated by pyrosequencing ("technical replicates") are shown in **Supplementary Figure 3**.

For our 359 genes with tissue type specific CpG methylation, their expression patterns in the 21 normal tissues are known (GEO Expression Omnibus, GEO, http://www.ncbi.nlm.nih.gov/geo/, **Supplementary Methods**). Unsupervised clustering analysis of the expression of these 359 genes discriminates each normal tissue type, as the CpG methylation did, reinforcing the association between DNA methylation and transcriptional silencing of the neighboring gene for these targets (**Supplementary Figure 3**). Strikingly, the CpG sites for which methylation status was the most valuable for discriminating between tissue types were those located in non-CpG island 5'-ends (Fisher's exact test, $p=5.85e^{-49}$). These data support the long-standing hypothesis that most housekeeping genes contain CpG islands around their transcription start sites, while half of the tissue-specific genes have a CpG island at their 5'-ends and the other half are 5'-CpG poor (Illingworth and Bird, 2009). The top-scoring genes with defined organ-specific DNA methylation are listed in

Supplementary Table 4. The tissue-type-specific DNA methylation patterns, which are in line with previous observations in humans (Eckhardt et al., 2006; Shen et al., 2007; Christensen et al., 2009; Byun et al., 2009), also match the developmental layers in which the tissues originated (endoderm, mesoderm or ectoderm) (**Fig. 1a**), implying the existence of germ-layer-specific DNA methylation (Sakamoto et al., 2007). Interestingly, 49 CpG sites corresponding to 26 imprinted genes were also included in the assay (**Supplementary Figure 4**). We observed that CpG sites located outside differentially methylated regions (DMRs) (Dindot et al., 2009; Monk et al., 2010) behaved like the CpGs of non-imprinted genes in normal tissues: CpGs located within and outside CpG islands were unmethylated and methylated, respectively (**Supplementary Figure 4**). However, CpGs within DMRs were 50% methylated in all normal tissue types studied (**Supplementary Figure 4**).

Within the same tissue type, interindividual DNA methylation differences were minimal. For example, the DNA methylation deviation plot for the 1,322 CpG sites studied in leukocyte samples from 180 healthy donors showed little heterogeneity (**Figure 1b**). However, it is interesting to note that the main DNA methylation differences between individuals occurred at CpG sites located outside CpG islands in comparison to CpG island-associated CpG dinucleotides (Wilcoxon test, $p=3.52e^{-39}$) (**Figure 1b**). One interesting issue concerned the putative impact of aging on the DNA methylation patterns of normal tissues in humans (Christensen et al., 2009; Teschendorff et al., 2010; Rakyan et al., 2010) and mice (Maegawa et al., 2010). Our analysis of the leukocyte samples from the 180 healthy donors (**Figure 1b**) revealed sets of genes that were significantly hypermethylated (n = 43) or hypomethylated (n = 25) during the normal aging process (**Figure 1c and Supplementary Table 5**). Examples of age-specific CpG methylation further validated by pyrosequencing are shown in **Supplementary Figure 4**. It is encouraging to note that there are genes with age-related methylation found in our study that were also identified in the mentioned previous reports using the same 1,505 CpG platform (Christensen et al., 2009) or the 27,000 CpG microarray (Teschendorff et al., 2010; Rakyan et al., 2010). Among these, we can underline for the age-hypermethylated genes MYOD1 (Myogenic Differentiation Antigen 1) and for the age-hypomethylated genes representative examples include CARD15 (Caspase Recruitment

Domain-containing protein 15), ACVR1 (Activin Receptor Type I) and SOD3 (Superoxide Dismutase 3). Furthermore, we also found that the CpG hypermethylation events in aging were significantly more likely to occur in the promoters of those genes with enriched polycomb occupancy (Fisher's exact test, $p=3.83e^{-8}$; permutation p-value 0.0014) and the presence of bivalent histone domain (3mK4H3 + 3mK27H3) (Fisher's exact test, $p=9.03e^{-4}$; permutation p-value 0.0354) in embryonic stem cells (**Supplementary Figure 4**), as was recently suggested (Rakyan et al., 2010; Teschendorff et al., 2010).

In addition to the tissue-type-specific DNA methylation patterns, one group of normal cells had distinctive DNA methylation profiles: embryonic and adult stem cells (**Figure 1d**). Adult and embryonic stem cells both had DNA methylation fingerprints that did not resemble any of the differentiated primary normal tissues studied (**Fig. 1d**). Furthermore, we confirmed that the previously studied samples from multipotent adult stem cells (Aranda et al., 2009) had different DNA methylation fingerprints than pluripotent embryonic stem cells (**Fig. 1d**). Herein, we went further to show that induction of differentiation of both types of stem cells through different lineages produced DNA methylation fingerprints that resembled those present in the corresponding normal differentiated tissues, such as muscle or neuron (**Fig. 1d**). Interestingly, *in vitro*-differentiated material from adult and embryonic stem cells did not completely recapitulate the DNA methylation patterns present in the corresponding primary differentiated tissues and there were always deficiently methylated CpG sites. **Supplementary Table 6** provides examples of these in muscle and neuronal tissues. **Supplementary Figure 5** shows examples of tissue-specific CpG methylation, unachieved upon *in vitro* differentiation of stem cells and validated by pyrosequencing analysis.

DNA methylation fingerprint of human cancer

We studied next the DNA methylation fingerprints for 1,054 human tumorigenesis samples. Genetic and epigenetic alterations both contribute to cancer initiation and progression (Jones and Baylin, 2007; Esteller, 2008). One of the first epigenetic alterations found in human cancer was the global low level of DNA methylation in tumors compared with healthy tissue counterparts

(Feinberg et al., 1983). Global DNA hypomethylation is accompanied by hypermethylation of CpG islands at specific promoter regions. Nowadays, hypermethylation of the CpG islands in the promoter regions of tumor-suppressor genes is also recognized as a major event in the origin of many cancers (Jones and Baylin, 2007; Esteller, 2008). Tumor suppressor genes disrupted by DNA methylation-associated transcriptional silencing in sporadic tumors include the retinoblastoma tumor suppressor gene (Rb), VHL (associated with von Hippel–Lindau disease), the cell cycle inhibitor $p16^{INK4a}$, hMLH1 (a homologue of MutL *Escherichia coli*) and BRCA1 (breast-cancer susceptibility gene 1) (Jones and Baylin, 2007; Esteller, 2008). Using candidate gene approaches and early epigenomic technologies, a CpG island hypermethylation profile of human primary tumors emerged that suggesting that a defining DNA hypermethylome could be assigned to each tumor type (Costello et al., 2000; Esteller et al., 2001; Ballestar and Esteller, 2008). Herein, we have analyzed the DNA methylation fingerprints of 1,054 human tumorigenesis samples, including 855 primary malignancies (611 solid tumors from 19 tissue types and 244 hematological malignancies), 50 metastatic lesions, 25 premalignant lesions, 82 cancer cell lines and 42 cancers of unknown primary origin (CUPs) (**Supplementary Table 1**). The DNA methylation map that emerges shows a tumor-type-specific profile characterized by the progressive gain of CpG methylation within CpG island-associated promoters and a cumulative loss of CpG methylation outside CpG islands in the different steps of tumorigenesis.

First, unsupervised clustering of the DNA methylation profiles obtained from the 855 primary tumors demonstrated that each type of malignancy had its own aberrant DNA methylation landscape (**Figure 2a**). From a quantitative standpoint, 1,003 CpG sites (76% of the 1,322 validated CpGs) had significantly different methylation levels between tumor types (Kruskal-Wallis rank sum test, $p<2.2e^{-16}$). The distinction of primary tumors by their tissue of origin was maintained even when we subtracted the tissue-type specific DNA methylation described above (511 CpG sites, **Supplementary Table 4**) from the analysis of the DNA methylation profiles for each normal tissue (**Fig. 2b**). Comparing each tumor type with its corresponding normal tissue, 729 CpG sites (55% of the 1,322 CpGs) showed differential DNA methylation. Using these tumor/normal

differentially methylated CpG sites, overall human primary tumors were characterized by increased levels of CpG dinucleotide methylation: 68% (n = 496) were hypermethylated and 32% (n = 233) were hypomethylated (t test, $p=3.521e^{-5}$) **(Figure 2c)**. Most importantly, the location of these DNA methylation events differed: CpG dinucleotide hypermethylation occurred within CpG islands (78%) while CpG hypomethylation was present in 5'-ends of non-CpG island genes (78%) (Fisher's exact test, $p=2.59e^{-47}$; permutation p-value <0.001) **(Figure 2c)**. A DNA methylation deviation plot for the 1,322 CpG sites studied in all normal primary tissues (n = 390) vs. all primary tumors (n = 855) shows the hypermethylated CpG sites within CpG islands and hypomethylated CpG sites outside CpG islands observed in the malignancies (**Figure 2c**) (Paired Wilcoxon test $p<2.2e^{-16}$). CpG sites with cancer-specific differential methylation according to tumor type in comparison with their corresponding normal tissue are provided in **Supplementary Table 7**. Examples of cancer type-specific CpG methylation further validated by pyrosequencing are shown in **Supplementary Figure 6**. Those CpG sites with highly specific methylation changes occurring only in one tumor type are shown in **Supplementary Table 8.** Interestingly, we also confirmed the previous observation (Schlesinger et al., 2007; Ohm et al., 2007; Widschwendter et al., 2007) that the CpG hypermethylation events in cancer were significantly more likely to occur in the promoters of those genes with enriched polycomb occupancy (Fisher's exact test, $p=5.03e^{-6}$; permutation p-value 0.0012) and the presence of bivalent histone domains (3mK4H3 + 3mK27H3) (Fisher's exact test, $p=5.97e^{-4}$; permutation p-value 0.0278) in embryonic stem cells (**Supplementary Figure 6**). We also found evidence to reinforce the link between the 5'-end CpG methylation and transcriptional silencing (Jones and Baylin 2007; Esteller 2008) by developing expression microarray studies (**Supplementary Methods**) in the 19 primary colorectal tumors from which we had obtained the DNA methylation profiles. We observed that the median expression of all the CpG hypermethylation-associated genes was significantly lower than in those CpG hypomethylation-linked genes (Kruskal-Wallis test, $p=1.56e^{-8}$) **(Supplementary Figure 6)**.

For our largest set of samples with paired normal-tumor tissues from the same patient (41 cases of colorectal cancer), we observed that of the 1,322

CpG sites studied, CpG dinucleotides within CpG island promoters became significantly more DNA-methylated in 79% of cases (34 of 43 normal/tumor pairs) (Wilcoxon test, $p=2.47e^{-7}$), while CpGs located in non-CpG island promoters more commonly underwent DNA hypomethylation events, in 51% of cases (22 of 43 normal/tumor pairs) (Wilcoxon test, $p = 0.001$). If we consider the colorectal tumor population as a whole, in 68% of cases (28 of 41) the primary malignancy gained CpG dinucleotide methylation within promoter CpG islands and non-CpG island promoters, while in 15% of tumors (6 of 41) the gain of CpG island methylation occurred in a context of loss of promoter non-CpG island methylation (**Figure 3a**). Interestingly, 17% of cases (7 of 41) featured a loss of methylation in both promoter CpG islands and non-CpG island promoters (**Figure 3a**). Thus, the presence of hypermethylation of promoter CpG islands appears to be a common hallmark of human tumors, but there are subsets of cancers that present other DNA methylation profiles at promoter CpG sites that suggest additional and complex aberrant DNA methylation pathways in tumorigenesis. For example, the possibility that DNA hypomethylation events at CpGs located in non-CpG island promoters, typical of genes with restricted tissue-specific expression (Illingworth and Bird, 2009), can cause a loss of cellular identity in transformed cells is worth further investigation.

As cancer cell lines are a major tool in biomedical research, we next examined how the DNA methylation profiles of cell lines differ from those of the primary tumor types. The analyses of the DNA methylation fingerprints of 82 human cancer cell lines representing 14 tumor types (**Supplementary Table 1**) showed that, overall, they preserved their original cancer type-specific profile and underwent an increase in the levels of CpG dinucleotide methylation in comparison with the corresponding normal tissues (Paired Wilcoxon test, $p<2.2e^{-16}$) (**Supplementary Figure 7**), as occurs with most primary tumors. Examples of CpG methylation in cancer cell lines further validated by pyrosequencing are shown in **Supplementary Figure 7.** In the same line as primary malignancies, the hypermethylated CpG sites in cancer cell lines occurred significantly more often within CpG islands (**Supplementary Figure 7**), while CpG hypomethylation events mainly happened around transcription start sites that did not contain a CpG island (Paired Wilcoxon test, $p<2.2e^{-16}$)

(**Supplementary Figure 7**). However there were qualitative and quantitative differences. First, human cancer cell lines had significantly greater hypermethylation of promoter CpG islands and non-CpG island promoters (Paired Wilcoxon test, $p<2.2e^{-16}$) (**Supplementary Figure 7**). At this stage, we cannot distinguish whether these greater changes are associated with the *in vitro* growth of these cells over many years, or if the DNA methylation changes were more detectable because there was no contaminating normal tissue, as is the case in primary tumors. Second, there are a set of specific CpG sites that only undergo differential DNA methylation in cancer cell lines (**Supplementary Table 9**) that enable them to be classified into a distinct clustering arm in the unsupervised analysis (**Figure 3b**). We further tested the association between hypermethylated CpGs at the 5'-ends and transcriptional silencing of the corresponding gene by treating five cancer cell lines (SW480, HN-011A, HN-011B, IGR37 and IGR39) with the DNA demethylating agent 5'-aza-2'-deoxycytidine, followed by gene expression microarray analysis (**Supplementary Methods**). We observed that while genes with associated hypermethylated CpGs had a low median expression compared with their corresponding normal tissues, upon treatment with the hypomethylating agent their expressions were restored **(Supplementary Figure 8).**

The comprehensive collection of human tumorigenesis samples studied here allowed us to address two other interesting aspect of cancer epigenetics: timing and progression. For genetic changes it is well known that there is an accumulation of genetic events that drive the carcinogenesis process from the healthy tissue to early premalignant lesions and finally to established full-blown tumors and metastasis, as exemplified by colorectal tumorigenesis (Fearon and Vogelstein, 1990). Candidate gene approaches and limited epigenomic strategies have also indicated that this could be a pathway leading to aberrant DNA methylation changes (Fraga et al., 2004). Our analysis of the DNA methylation signatures in progressive samples of three different tumorigenesis pathways (colon, breast and endometrial cancers) demonstrated the increasing degree of CpG dinucleotide methylation within promoter CpG islands and a loss of CpG methylation outside CpG islands in consecutive steps (**Figure 3c**). The DNA methylation deviation plot for the 1,322 CpG sites in colorectal adenomas vs. primary colorectal tumors, breast hyperplasias vs. primary breast tumors

and endometrial hyperplasias vs. primary endometrial carcinomas demonstrated that the full-blown tumors had significantly greater hypermethylation of promoter CpG islands in association with the loss of CpG methylation in non-CpG islands than their corresponding premalignant lesions (Paired Wilcoxon test, $p<2.2e^{-16}$) (**Figure 3c**). Most importantly, for colorectal tumors where we had DNA from brain metastasis available, these distant metastasis lesions achieved higher levels of promoter CpG island hypermethylation and lower levels of non-CpG island methylation than the primary colon malignancies (Paired Wilcoxon test, $p<2.2e^{-16}$), suggesting that these pathological entities are the final stages of the disease. In fact, the DNA methylation unsupervised clustering analyses of primary tumors, local liver metastases and distant brain metastases from the same colorectal cancer patient showed that there were specific hypermethylated CpGs in the brain metastases (**Supplementary Table 10 and Figure 3d**). Examples of specific CpG methylation in the brain metastasis of colorectal tumors validated by pyrosequencing are shown in **Supplementary Figure 8**. 90% of cancer deaths are attributable to the development of metastasis (Mehlen and Puisieux, 2006), so these findings might have a translational value for the prediction of the metastatic capacity of a particular tumor, as has recently been shown for hypermethylated microRNA loci (Lujambio et al., 2008), and it might be a useful molecular marker in the decision process for the medical and surgical intervention in the disease.

The DNA methylation fingerprints of human cancer obtained in our study can also provide additional important molecular diagnostic and prognostic biomarkers for the management of neoplasias. One example we have assessed is the case of the clinical entities classified as Cancers of Unknown Primary Origin (CUPs). These are patients that present metastatic diseases for which the primary site cannot be found despite standard investigation. The median survival in randomized studies of these patients is extremely poor (Abbruzzese et al., 1995), but if it were possible to predict the primary tumor site, the patient could be treated with a site-specific program, potentially resulting in better survival than that provided by non-specific treatment, for which the current median is only 7 months (Greco and Pavlici, 2009). We have analyzed the DNA methylation fingerprints of 42 CUPs and compared the DNA methylation

landscapes obtained with those from the aforementioned human malignancy collection where the original tissue type was known. We were able to assign a given tumor type for these CUPs in 69% (29 of 42) of cases using L1-regularized logistic regression with misclassification (R, version 2.10) to create a prediction heatmap (**Figure 3e**). A proposed foster primary in these 29 cases was also achieved by conventional clustering analysis (**Supplementary Figure 8**). Most importantly, the tumor type prediction of the CUPs based on the DNA methylation analyses was fullly confirmed in 78% of cases (7 of 9) for which detailed pathological analysis developed at a later stage in a blind fashion was able to provide a diagnosis. We might also conclude that the remaining 31% (13 of 42) of the studied CUP cases did not represent any of the 19 tumor types included in our analysis (**Supplementary Table 1**). The three most common tumor types present in the DNA methylation-assigned CUPs were colorectal cancer (34%, 10 of 29), non-small cell lung cancer (17%, 5 of 29) and breast tumors (17%, 5 of 29). These cases are particularly interesting because the introduction of targeted therapies, such as treatment with epidermal growth factor receptor (EGFR) antibodies in colorectal cancer, small-molecule inhibitors for EGFR mutations in lung adenocarcinoma and more personalized chemotherapy options for breast cancer as a function of the hormonal and ERBB2 receptor status have improved the outcome of these patients (Harris and McCormick, 2010). Thus, it is tempting to propose that the prediction of a foster primary site for CUPs based on the DNA methylation profiles might identify a more specific treatment regimen for these patients that would improve their quality of life and survival.

DNA methylation fingerprint of human non-cancerous human diseases

We also analyzed the DNA methylation profiles for 150 non-cancerous human diseases. Although most of the aberrant DNA methylation patterns described in human disease have been reported for cancer, there is no reason to believe that disrupted DNA methylation signatures are not present, and might drive other common human diseases (Feinberg et al., 2007), such as neurological (Urdinguio et al., 2009), cardiovascular (Gluckman et al., 2009) and autoimmune (Richardson, 2007) disorders. The data on DNA methylation

changes outside cancer are still scarce, but this could be more likely because of the small number of studies devoted to these pathologies than because DNA methylation disruption is genuinely of little importance in the origin and progression of these diseases. To address this issue, we analyzed the corresponding target tissues of 150 non-cancerous human diseases, including cerebral cortex lesions from Alzheimer's (n = 11) and dementia with Lewy bodies (n = 13), atherosclerotic lesions from the aorta (n = 18), skeletal muscle from myopathies (n = 17), leukocytes from autoimmune disorders (n = 21) and other non-tumoral diseases and tissues (n = 70) (**Supplementary Table 1**).

One of the most striking observations was that the described non-tumoral diseases in an unsupervised clustering had a distinct DNA methylation pattern, even if the tissue-specific CpG methylated sites were not included in the analysis (**Figure 4a**). In the cases of dementia with Lewy bodies (**Figure 4b**) and systemic lupus erythematosus (**Supplementary Figure 9**) the DNA methylation patterns obtained from the 1,322 CpG sites distinguished them from their corresponding normal tissues. Most importantly, the corresponding distinctions between brain samples of dementia with Lewy bodies vs. normal brain; and leukocytes of lupus patients vs. healthy donor samples was exclusively associated with CpG hypomethylation events in the disease tissue (**Supplementary Table 11**). Examples of dementia with Lewy bodies-specific CpG hypomethylation further validated by pyrosequencing are shown in **Supplementary Figure 9**. Interestingly, it has been recently described the sequestration of DNA methyltransferase 1 (DNMT1) in the cytoplasm of neurons from patients affected by dementia with Lewy bodies (Desplats et al., 2011), a mechanism that could explain the hypomethylation events observed in this disease using our approach. Related to the lupus patients, it is noteworthy to consider that these samples were also previously analyzed using the same 1,505 CpG array to search for DNA methylation differences between monozygotic twins (Javierre et al., 2010). Herein, they were studied in a more stringent manner because they were compared to a new large set of normal leukocytes (n=180) and with a higher cut-off value for methylation. Among the lupus-common genes derived from both studies, it is relevant to mention the hypomethylation event targeting PI3 (Proteinase Inhibitor 3), a protein that has been involved in psoriasis with an autoimmune component (Tjabringa et al.,

2008). With the CpG array used we were unable to find any significant difference between brain samples from Alzheimer's patients (**Figure 4b**), aorta samples from atherosclerotic lesions (**Supplementary Figure 9**), myopathies (data not shown) and their respective normal tissues.

The DNA methylation profiles obtained from the aforementioned non-cancer disorders were distinct from those observed in tumors originating from the same cell type. Dementia with Lewy bodies' patients had CpG site methylation patterns that distinguished them not only from normal brain (**Figure 4b**), but also from neuroectodermal tumors, such as glioma and neuroblastoma (**Figure 4c**). Interestingly, brain samples from dementia with Lewy bodies' patients were closer, from a DNA methylation fingerprint perspective, to neuroblastomas than to gliomas (**Figure 4c**), a characteristic that might be associated with the different cell biology of the disorders. Although in dementia associated with Alzheimer's disease there is a high grade of neuronal cell death that causes an over-representation of glia cells in the studied samples (gliosis) (Jellinger and Stadelmann, 2001; Teaktong et al., 2003); in the dementia with Lewy bodies' brain there is not such massive neuronal cell death (Jellinger and Stadelmann, 2001; Teaktong et al., 2003) and the DNA methylation profiles observed resembled those found in neuron-enriched samples, such as neuroblastomas. In this regard, the existence of different DNA methylation patterns among brain regions with different cell composition has also been suggested (Ladd-Acosta et al., 2007). Distinct DNA methylation profiles for non-malignant and malignant disorders originating from the same cell type also occur for leukocytes of lupus patients displaying DNA methylation profiles that are different from those present in healthy donors or in leukemias (**Supplementary Figure 9**).

Overall, these findings suggest that few specific DNA methylation changes in non-cancerous human diseases could be responsible for the observed phenotypes of these entities; they nevertheless merit further attention. Most importantly, the specific DNA methylation changes found in the described disorders occurred in clear contrast to human cancer, where the DNA methylation profile undergoes a wide-ranging, global change characterized by the gain of promoter CpG island methylation and loss of non-CpG island methylation. These results underlie the multifactorial nature of human cancer

that involves epigenetic “hits” in almost all known cellular pathways, exemplified by the aberrant DNA methylation fingerprints obtained here.

Discussion

The disruption of the DNA methylation patterns is emerging a common feature of human disease (Portela and Esteller, 2010) where cancer is the disorder where most of the studies have been focused (Jones and Baylin 2007; Esteller 2008). From the initial studies looking at single locus, we have now available a wide range of epigenomic techniques to study multiple CpG sites in the human genome. In addition to methods that isolate methylated fractions of the genome by methylation-sensitive restriction (Lippman et al. 2005; Irizarry et al., 2008), immunoprecipitation with a methylcytosine (Weber et al. 2005; Keshet et al. 2006; Weber et al., 2007; Down et al., 2008) or methyl-CpG binding domain antibody (Ballestar et al., 2003; Rauch et al., 2009) and the genome-wide bisulfite genomic sequencing approaches (Lister et al., 2009; Li et al., 2009), it is worth to highlight the DNA methylation bead microarrays (Bibikova et al., 2006). This approach has the advantage that it can be used in a common standard manner by different laboratories around the world with similar bioinformatic packages and the raw data can be user-friendly deposited and shared. Herein, using the first version of the DNA methylation bead microarray, that included 1,505 CpG sites corresponding to 808 genes, we have studied the largest collection of human samples to date, 1,628, that included 424 normal tissues, 1,054 tumorigenic samples and 150 non-cancerous disorders. Our data provide new clues about the DNA methylation profiles present in normal and disease-associated tissues and it also expand and confirm previous reports in this area obtained using the same platform (Christensen et al., 2009; Byun et al., 2009; Aranda et al., 2009; Javierre et al., 2010) or a second DNA methylation bead microarray that includes 27,000 CpG sites (Rakyan et al., 2010; Teschendorff et al., 2010; Nagae et al., 2011). In normal cells, the derived picture reinforces the role of methylation in non-CpG island 5’-ends to determine tissue-specific expression, the shift in the DNA methylation landscape from pluripotent to differentiated cells and the existence of a DNA

methylation drift associated with aging. For transformed cells, the study demonstrate that tumors undergo mostly a progressive CpG hypermethylation within CpG islands while CpG hypomethylation occurs in 5'-ends of non-CpG island genes. For other human disorders, such as dementia with Lewy bodies and lupus, we show that they also possess a particular DNA methylation fingerprinting that it is mainly characterized by CpG hypomethylation events. One extra value of the current study it is that not only provide new DNA methylation markers for all the described normal and pathological setting, but it also validate previous results in aging (Christensen et al., 2009; Rakyan et al., 2010; Teschendorff et al., 2010), tissue-specificity (Eckhardt et al., 2006; Byun et al., 2009; Christensen et al., 2009) or lupus (Javierre et al., 2010). Furthermore, the deposited data for the 1,628 human samples (http://www.ncbi.nlm.nih.gov/geo accession number GSE28094) can be a value resource for further biocomputational and meta-analysis studies.

Overall, the goal of the research described here was to examine comprehensively human DNA methylation profiles from an extremely extensive range of samples that covers physiological changes (across different tissue types, sex, age, geography, differentiation vs. stemness, primary vs. cell culture, etc.) and human diseases (cancer and common non-tumoral diseases, such as neurological, cardiovascular and autoimmune disorders). The results obtained indicate that different DNA methylation fingerprints are observed in most of the described conditions, cancer samples being the result of the most extreme type of DNA methylation change observed, in which a profile of an increased degree of CpG dinucleotide methylation within promoter CpG islands and a loss of CpG methylation outside CpG islands is a common hallmark, as described above. A DNA methylation signature that becomes more distorted as the disease progresses, but that can provide potentially relevant clues for improving disease management for these patients, such as we have demonstrated for the CUP cases.

We would like to underscore the relevance of the CUP DNA methylation fingerprints. In spite of the increasing sophistication in the diagnostic tools for malignancies, deaths due to CUP were estimated to be 45,230 in 2007 in USA (American Cancer Society, 2007). CUPs have an incidence of 6% among all malignancies and in 25% of cases, the primary site cannot be identified even on

postmortem examination (American Cancer Society, 2007). The inability to identify the primary site of the cancer and the impossibility to provide the right treatment has a large impact in the expected clinical outcome of these patients. Herein, the obtention of DNA methylation fingerprints for 1,054 tumorigenic samples allowed the classification according to cancer-type of almost 70% of the studied CUPs, a result that can make a difference in the prognosis of these patients. This is just an example of the possible translational use of the provided DNA methylation profiles. Other uses might follow and they will require further development, such as our finding of a distinct DNA methylation fingerprint between local liver metastases and distant brain metastases derived from colorectal tumors that might suggest the use of DNA methylation patterns to predict the metastatic spectrum of a given cancer. We would also like to highlight another promising step in the clinical benefit direction by the recent finding of 27,000 CpG site DNA methylation profiles in blood that are associated with bladder cancer risk (Marsit et al., 2011).

One obvious limitation of our approach is the level of resolution, since only 1,505 CpG sites were interrogated. The increasing number of studies developed and underway using the 27,000 CpG site platform and the future reports using the new 450K CpG site microarray will be useful to further validate and complement the obtained DNA methylation profiles. We can only imagine how the firm, automatic and affordable establishment of whole genome sequencing of complete human DNA methylomes (Lister et al., 2009; Li et al., 2010) will yield further knowledge about the role of DNA methylation in cellular identity and its loss in disease. Even so, the 1,628 DNA methylation fingerprints described herein, and displayed by tissue type and disease in **Figure 5**, are a promising starting point for understanding the variation of human DNA methylation over a range of normal and pathological conditions.

Methods

Filtering of probes and samples

Although the Illumina GoldenGate® Assay assay by Illumina is an established highly reproducible method for DNA methylation detection, there is currently no standard procedure for post-filtering of probes and samples is commonly used. Before analyzing the methylation data, we excluded explored several ways of excluding possible sources of biological and technical biases that could have affected the and improving the accuracy of the results. Every beta value in the GoldenGate platform is accompanied by a detection p-value. We based the criteria of filtering on these p-values reported by the assay. We examined two aspects of filtering out probes and samples based on the detection p-values, selecting a threshold and a cutoff. Our analyses indicated that a threshold value of 0.01 allows a clear distinction to be made between reliable and unreliable beta values. We selected the cutoff value as 5%. Following this criterion, we first removed all probes with detection p-values > 0.01 in 5% or more of the samples. As a second step, we removed all samples with detection p-values > 0.01 in 5% or more of their (remaining) probes. In total, 130 probes and 87 samples were removed. We also checked for and removed consistently unmethylated and methylated probes. We ignored all cell line samples and focused on the remaining 1521 (primary tissue) samples. All probes exhibiting a degree of methylation < 0.25 for all primary tissue samples were considered to be consistently unmethylated. Similarly, probes with a degree of methylation > 0.75 for all primary tissue samples were considered to be consistently methylated. We identified nine consistently unmethylated probes; none of the probes fitted our definition for being consistently methylated. A known biological factor is that one copy of chromosome X is methylated in women (Reik and Lewis 2005) and therefore, we decided to identify and remove all probes with prominent gender-specific methylation, in order to avoid hidden bias in the subsequent analyses. We considered the set of 1,271 samples with gender information; approximately half of them were female. We defined a probe to be gender-specific if (1) the probe showed a significant differential methylation between the two sample groups, as determined by the Mann-Whitney U test

with FDR correction, and (2) the mean methylation degrees of females and males for this probe differed by at least 0.17 (a limitation of the GoldenGate assay). After excluding 130 probes that were not of sufficient quality, nine that were consistently unmethylated and 44 that were gender-specific, 1,322 probes were available for further statistical analyses.

Analysis of differentially methylated probes

The large cohort of heterogeneous methylation profiles allows us to identify differentially methylated probes under a variety of scenarios. We analyzed different groups of tissue samples separately (normal primary tissues, cancerous and non-cancerous diseases and cancer cell lines). We performed all statistical analyses using the R environment for statistical computing (version 2.10; http://www.R-project.org.) . Further explanation about detection of differentially methylated probes and genes in each scenario, statistical analyses and graphical representations are provided in Supplemental Methods.

Pyrosequencing

Pyrosequencing assays were designed in order to analyze and validate the results obtained from the array under different scenarios. Sodium bisulfite modification of 0.5 µg of genomic DNA isolated from different tissues was carried out with the EZ DNA Methylation™ Kit (Zymo Research Corporation) following the manufacturer's protocol. Bisulfite-treated DNA was eluted in 15-µl volumes with 2 µl used for each PCR. The set of primers for PCR amplification and sequencing were designed with a specific program (PyroMark assay design version 2.0.01.15). Primer sequences were designed to hybridize with CpG-free sites to ensure methylation-independent amplification. PCR was performed with primers biotinylated to convert the PCR product to single-stranded DNA templates. We used the Vacuum Prep ToolTM (Biotage) to prepare single-stranded PCR products according to the manufacturer’s instructions. Pyrosequencing reactions and quantification of methylation were performed in a PyroMark Q24 System version 2.0.6 (Qiagen). Graphs of methylation values show bars identifying CpG sites with values from 0% (white) to 100% (black).

Classification of CUPs

We used the advanced method L1-regularized logistic regression with misclassification to classify the 42 CUP samples in our dataset into one of the known cancer types. By classifying a CUP, this classifier gives probabilities (values between 0 and 1) for every known cancer type. A CUP prediction heatmap was derived in R (version 2.1.0) (Figure 3e). The CUP samples were selected on the basis of having a probability of being ascribed to a specific tumor type over 30%. The arrangement of the samples in the heatmap was established by (1) ordering the tumor types by the number of CUPs ascribed to each one, and (2) within each tumor type, ranking the CUPs from the highest to lowest probability of ascription.

Expression data analysis

CEL files containing normal tissue gene expression data were downloaded from GEO database. Data series, samples and analyses procedures are detailed in Supplementary Methods.

Enrichment of PcG-marks and bivalent domains in different methylation groups

The presence of PcG-marks and bivalent domains in different methylation groups was compared using Fisher's exact test. In addition to Fisher's exact test, we calculated permutation-based p-values to account for interdependencies between the methylation states of different CpGs. Briefly, we performed Fisher's exact test in 104 random reassignments of the studied samples and calculated the proportion of resulting p-values that is lower than or equal to the originally obtained one. A genome-wide map of Polycomb target genes and 3mK4H3/3mK27H3-enriched genes in ESCs is available as supplemental material of the articles by Lee et al. (Lee et al. 2006) and Pan et al. (Pan et al. 2007), respectively.

Human cancer cell lines and expression upon 5-aza-2´-deoxycytidine treatment

Five cancer cell lines SW480 (colon), HN-011A and HN-011B (esophagus) and IGR37 and IGR39 (melanoma) were grown in DMEM medium supplemented with 4 mM glutamine, 10% FBS and 100 units/ml penicillin/streptomycin at

37ºC/5% CO2. All cell lines were treated with 1 µM 5-aza-2´-deoxycytidine (Sigma) for 72 h. Total RNA was isolated from all cell lines before and after 5-aza-2´-deoxycytidine treatment, by Trizol extraction (Invitrogen), and 5 µg were hybridized on the Affymetrix Human GeneChip U133 Plus 2.0 expression array (Affymetrix, Santa Clara, CA). Expression data were normalized and analyzed following the same procedures described in Supplementary Methods.

References

Abbott A. 2010. Project set to map marks on genome. *Nature* **463:** 596-597.

Abbruzzese JL, Abbruzzese MC, Lenzi R, Hess KR, Raber MN. 1995. Analysis of a diagnostic strategy for patients with suspected tumors of unknown origin. *J Clin Oncol* **13:** 2094-2103.

American Cancer Society. Statistics for 2007. *American Cancer Society Statistics*. Available at http://www.cancer.org/docroot/stt/stt_0.asp.

Aranda P, Agirre X, Ballestar E, Andreu EJ, Román-Gómez J, Prieto I, Martín-Subero JI, Cigudosa JC, Siebert R, Esteller M, et al. 2009. Epigenetic signatures associated with different levels of differentiation potential in human stem cells. *PLoS One* **4**: e7809.

Ballestar E, Esteller M. 2008. SnapShot: the human DNA methylome in health and disease. *Cell* **135:** 1144-1144 e1141.

Ballestar E, Paz MF, Valle L, Wei S, Fraga MF, Espada J, Cigudosa JC, Huang TH, Esteller M. 2003. Methyl-CpG binding proteins identify novel sites of epigenetic inactivation in human cancer. *Embo J* **22:** 6335-6345.

Bernstein BE, Meissner A, Lander ES. 2007. The mammalian epigenome. *Cell* **128:** 669-681.

Bibikova M, Lin Z, Zhou L, Chudin E, Garcia EW, Wu B, Doucet D, Thomas NJ, Wang Y, Vollmer E et al. 2006. High-throughput DNA methylation profiling using universal bead arrays. *Genome Res* **16:** 383-393.

Bonetta L. 2008. Epigenomics: Detailed analysis. *Nature* **454:** 795-798.

Byun HM, Siegmund KD, Pan F, Weisenberger DJ, Kanel G, Laird PW, Yang AS. 2009. Epigenetic profiling of somatic tissues from human autopsy specimens identifies tissue- and individual-specific DNA methylation patterns. *Hum Mol Genet* **18:** 4808-4817.

Cantor RM, Lange K, Sinsheimer JS. 2010. Prioritizing GWAS results: A review of statistical methods and recommendations for their application. *Am J Hum Genet* **86:** 6-22.

Cokus SJ, Feng S, Zhang X, Chen Z, Merriman B, Haudenschild CD, Pradhan S, Nelson SF, Pellegrini M, Jacobsen SE. 2008. Shotgun bisulphite sequencing of the Arabidopsis genome reveals DNA methylation patterning. *Nature* **452:** 215-219.

Costello JF, Fruhwald MC, Smiraglia DJ, Rush LJ, Robertson GP, Gao X, Wright FA, Feramisco JD, Peltomaki P, Lang JC et al. 2000. Aberrant CpG-island methylation has non-random and tumour-type-specific patterns. *Nat Genet* **24:** 132-138.

Christensen BC, Houseman EA, Marsit CJ, Zheng S, Wrensch MR, Wiemels JL, Nelson HH, Karagas MR, Padbury JF, Bueno R et al. 2009. Aging and environmental exposures alter tissue-specific DNA methylation dependent upon CpG island context. *PLoS Genet* **5:** e1000602.

Das R, Hampton DD, Jirtle RL. 2009. Imprinting evolution and human health. *Mamm Genome* **20:** 563-572.

Desplats P, Spencer B, Coffee E, Patel P, Michael S, Patrick C, Adame A, Rockenstein E, Masliah E. 2011. {alpha}-Synuclein sequesters Dnmt1 from the nucleus: a novel mechanism for epigenetic alterations in Lewy body diseases. *J Biol Chem* **286**: 9031-9037.

Dindot SV, Person R, Strivens M, Garcia R, Beaudet AL. 2009. Epigenetic profiling at mouse imprinted gene clusters reveals novel epigenetic and genetic features at differentially methylated regions. *Genome Res* **19:** 1374-1383.

Doi A, Park IH, Wen B, Murakami P, Aryee MJ, Irizarry R, Herb B, Ladd-Acosta C, Rho J, Loewer S et al. 2009. Differential methylation of tissue- and cancer-specific CpG island shores distinguishes human induced pluripotent stem cells, embryonic stem cells and fibroblasts. *Nat Genet* **41:** 1350-1353.

Down TA, Rakyan VK, Turner DJ, Flicek P, Li H, Kulesha E, Graf S, Johnson N, Herrero J, Tomazou EM et al. 2008. A Bayesian deconvolution strategy for immunoprecipitation-based DNA methylome analysis. *Nat Biotechnol* **26:** 779-785.

Eckhardt F, Lewin J, Cortese R, Rakyan VK, Attwood J, Burger M, Burton J, Cox TV, Davies R, Down TA et al. 2006. DNA methylation profiling of human chromosomes 6, 20 and 22. *Nat Genet* **38:** 1378-1385.

Esteller M. 2007. Cancer epigenomics: DNA methylomes and histone-modification maps. *Nat Rev Genet* **8:** 286-298.

Esteller M. 2008. Epigenetics in cancer. *N Engl J Med* **358:** 1148-1159.

Esteller M, Corn PG, Baylin SB, Herman JG. 2001. A gene hypermethylation profile of human cancer. *Cancer Res* **61:** 3225-3229.

Fearon ER, Vogelstein B. 1990. A genetic model for colorectal tumorigenesis. *Cell* **61:** 759-767.

Feinberg AP. 2007. Phenotypic plasticity and the epigenetics of human disease. *Nature* **447:** 433-440.

Fernandez AF, Rosales C, Lopez-Nieva P, Grana O, Ballestar E, Ropero S, Espada J, Melo SA, Lujambio A, Fraga MF et al. 2009. The dynamic DNA methylomes of double-stranded DNA viruses associated with human cancer. *Genome Res* **19:** 438-451.

Fraga MF, Ballestar E, Paz MF, Ropero S, Setien F, Ballestar ML, Heine-Suner D, Cigudosa JC, Urioste M, Benitez J et al. 2005. Epigenetic differences arise during the lifetime of monozygotic twins. *Proc Natl Acad Sci U S A* **102:** 10604-10609.

Fraga MF, Herranz M, Espada J, Ballestar E, Paz MF, Ropero S, Erkek E, Bozdogan O, Peinado H, Niveleau A et al. 2004. A mouse skin multistage carcinogenesis model reflects the aberrant DNA methylation patterns of human tumors. *Cancer Res* **64:** 5527-5534.

Frigola J, Song J, Stirzaker C, Hinshelwood RA, Peinado MA, Clark SJ. 2006. Epigenetic remodeling in colorectal cancer results in coordinate gene suppression across an entire chromosome band. *Nat Genet* **38:** 540-549.

Gluckman PD, Hanson MA, Buklijas T, Low FM, Beedle AS. 2009. Epigenetic mechanisms that underpin metabolic and cardiovascular diseases. *Nat Rev Endocrinol* **5:** 401-408.

Greco FA, Pavlidis N. 2009. Treatment for patients with unknown primary carcinoma and unfavorable prognostic factors. *Semin Oncol* **36:** 65-74.

Harris TJ, McCormick F. 2010. The molecular pathology of cancer. *Nat Rev Clin Oncol* **7:** 251-265.

Hemberger M, Dean W, Reik W. 2009. Epigenetic dynamics of stem cells and cell lineage commitment: digging Waddington's canal. *Nat Rev Mol Cell Biol* **10:** 526-537.

Humpherys D, Eggan K, Akutsu H, Hochedlinger K, Rideout WM, 3rd, Biniszkiewicz D, Yanagimachi R, Jaenisch R. 2001. Epigenetic instability in ES cells and cloned mice. *Science* **293:** 95-97.

Illingworth RS, Bird AP. 2009. CpG islands--'a rough guide'. *FEBS Lett* **583:** 1713-1720.

Irizarry RA, Ladd-Acosta C, Carvalho B, Wu H, Brandenburg SA, Jeddeloh JA, Wen B, Feinberg AP. 2008. Comprehensive high-throughput arrays for relative methylation (CHARM). *Genome Res* **18:** 780-790.

Irizarry RA, Ladd-Acosta C, Wen B, Wu Z, Montano C, Onyango P, Cui H, Gabo K, Rongione M, Webster M et al. 2009. The human colon cancer methylome shows similar hypo- and hypermethylation at conserved tissue-specific CpG island shores. *Nat Genet* **41:** 178-186.

Javierre BM, Fernandez AF, Richter J, Al-Shahrour F, Martin-Subero JI, Rodriguez-Ubreva J, Berdasco M, Fraga MF, O'Hanlon TP, Rider LG, et al. Changes in the pattern of DNA methylation associate with twin discordance in systemic lupus erythematosus. 2010. *Genome Res* **20**: 170-179.

Jellinger KA, Stadelmann C. 2001. Problems of cell death in neurodegeneration and Alzheimer's Disease. *J Alzheimers Dis* **3:** 31-40.

Jones PA AT, Baylin SB, Beck S, Berger S, Bernstein BE, Carpten JD, Clark SJ, Costello JF, Doerge RW, et al. 2008. Moving AHEAD with an international human epigenome project. *Nature* **454:** 711-715.

Jones PA, Baylin SB. 2007. The epigenomics of cancer. *Cell* **128:** 683-692.

Kaminsky ZA, Tang T, Wang SC, Ptak C, Oh GH, Wong AH, Feldcamp LA, Virtanen C, Halfvarson J, Tysk C et al. 2009. DNA methylation profiles in monozygotic and dizygotic twins. *Nat Genet* **41:** 240-245.

Keshet I, Schlesinger Y, Farkash S, Rand E, Hecht M, Segal E, Pikarski E, Young RA, Niveleau A, Cedar H et al. 2006. Evidence for an instructive mechanism of de novo methylation in cancer cells. *Nat Genet* **38:** 149-153.

Ku CS, Loy EY, Pawitan Y, Chia KS. 2010. The pursuit of genome-wide association studies: where are we now? *J Hum Genet* **55:** 195-206.

Kuehn BM. 2008. 1000 Genomes Project promises closer look at variation in human genome. *Jama* **300:** 2715.

Ladd-Acosta C, Pevsner J, Sabunciyan S, Yolken RH, Webster MJ, Dinkins T, Callinan PA, Fan JB, Potash JB, Feinberg AP. 2007. DNA methylation signatures within the human brain. *Am J Hum Genet* **81:** 1304-1315.

Lee TI, et al. Control of developmental regulators by Polycomb in human embryonic stem cells. Cell 125, 301-13 (2006).

Pan G, et al. Whole-genome analysis of histone H3 lysine 4 and lysine 27 methylation in human embryonic stem cells. Cell Stem Cell 1, 299-312 (2007).

Li Y, Zhu J, Tian G, Li N, Li Q, Ye M, Zheng H, Yu J, Wu H, Sun J et al. 2010. The DNA methylome of human peripheral blood mononuclear cells. *PLoS Biol* **8:** e1000533.

Lippman Z, Gendrel AV, Colot V, Martienssen R. 2005. Profiling DNA methylation patterns using genomic tiling microarrays. *Nat Methods* **2:** 219-224.

Lister R, Ecker JR. 2009. Finding the fifth base: genome-wide sequencing of cytosine methylation. *Genome Res* **19:** 959-966.

Lister R, O'Malley RC, Tonti-Filippini J, Gregory BD, Berry CC, Millar AH, Ecker JR. 2008. Highly integrated single-base resolution maps of the epigenome in Arabidopsis. *Cell* **133:** 523-536.

Lister R, Pelizzola M, Dowen RH, Hawkins RD, Hon G, Tonti-Filippini J, Nery JR, Lee L, Ye Z, Ngo QM et al. 2009. Human DNA methylomes at base resolution show widespread epigenomic differences. *Nature* **462:** 315-322.

Maegawa S, Hinkal G, Kim HS, Shen L, Zhang L, Zhang J, Zhang N, Liang S, Donehower LA, Issa JP. 2010. Widespread and tissue specific age-related DNA methylation changes in mice. *Genome Res* **20:** 332-340.

Marsit CJ, Koestler DC, Christensen BC, Karagas MR, Houseman EA, Kelsey KT. 2011. DNA methylation array analysis identifies profiles of blood-derived DNA methylation associated with bladder cancer. *J Clin Oncol* **29**:1133-1139.

Mehlen P, Puisieux A. 2006. Metastasis: a question of life or death. *Nat Rev Cancer* **6:** 449-458.

Meissner A, Mikkelsen TS, Gu H, Wernig M, Hanna J, Sivachenko A, Zhang X, Bernstein BE, Nusbaum C, Jaffe DB et al. 2008. Genome-scale DNA methylation maps of pluripotent and differentiated cells. *Nature* **454:** 766-770.

Michaud EJ, van Vugt MJ, Bultman SJ, Sweet HO, Davisson MT, Woychik RP. 1994. Differential expression of a new dominant agouti allele (Aiapy) is correlated with methylation state and is influenced by parental lineage. *Genes Dev* **8:** 1463-1472.

Monk D. 2010. Deciphering the cancer imprintome. *Brief Funct Genomics* **9:** 329-339.

Nagae G, Isagawa T, Shiraki N, Fujita T, Yamamoto S, Tsutsumi S, Nonaka A, Yoshiba S, Matsusaka K, Midorikawa Y, I et al. 2011. Tissue-specific demethylation in CpG-poor promoters during cellular differentiation. *Hum Mol Genet* In Press.

Ohm JE, McGarvey KM, Yu X, Cheng L, Schuebel KE, Cope L, Mohammad HP, Chen W, Daniel VC, Yu W et al. 2007. A stem cell-like chromatin pattern may predispose tumor suppressor genes to DNA hypermethylation and heritable silencing. *Nat Genet* **39:** 237-242.

Lee TI, Jenner RG, Boyer LA, Guenther MG, Levine SS, Kumar RM, Chevalier B, Johnstone SE, Cole MF et al. 2006. Control of developmental regulators by Polycomb in human embryonic stem cells. *Cell* **125**: 301-313.

Pan G, Tian S, Nie J, Yang C, Ruotti V, Wei H, Jonsdottir GA, Stewart R, Thomson JA.. 2007. Whole-genome analysis of histone H3 lysine 4 and lysine 27 methylation in human embryonic stem cells. *Cell Stem Cell* **1:** 299-312.

Portela A, Esteller M. 2010. Epigenetic modifications and human disease. *Nat Biotechnol* **28**:1057-1068.

Rakyan VK, Down TA, Maslau S, Andrew T, Yang TP, Beyan H, Whittaker P, McCann OT, Finer S, Valdes AM et al. 2010. Human aging-associated DNA hypermethylation occurs preferentially at bivalent chromatin domains. *Genome Res* **20:** 434-439.

Rakyan VK, Hildmann T, Novik KL, Lewin J, Tost J, Cox AV, Andrews TD, Howe KL, Otto T, Olek A et al. 2004. DNA methylation profiling of the human major

histocompatibility complex: a pilot study for the human epigenome project. *PLoS Biol* **2:** e405.

Rauch TA, Wu X, Zhong X, Riggs AD, Pfeifer GP. 2009. A human B cell methylome at 100-base pair resolution. *Proc Natl Acad Sci U S A* **106:** 671-678.

Reik W, Lewis A. 2005. Co-evolution of X-chromosome inactivation and imprinting in mammals. *Nat Rev Genet* **6:** 403-410.

Richardson B. 2007. Primer: epigenetics of autoimmunity. *Nat Clin Pract Rheumatol* **3:** 521-527.

Sakamoto H, Suzuki M, Abe T, Hosoyama T, Himeno E, Tanaka S, Greally JM, Hattori N, Yagi S, Shiota K. 2007. Cell type-specific methylation profiles occurring disproportionately in CpG-less regions that delineate developmental similarity. *Genes Cells* **12:** 1123-1132.

Schlesinger Y, Straussman R, Keshet I, Farkash S, Hecht M, Zimmerman J, Eden E, Yakhini Z, Ben-Shushan E, Reubinoff BE et al. 2007. Polycomb-mediated methylation on Lys27 of histone H3 pre-marks genes for de novo methylation in cancer. *Nat Genet* **39:** 232-236.

Shen L, Kondo Y, Guo Y, Zhang J, Zhang L, Ahmed S, Shu J, Chen X, Waterland RA, Issa JP. 2007. Genome-wide profiling of DNA methylation reveals a class of normally methylated CpG island promoters. *PLoS Genet* **3:** 2023-2036.

Siva N. 2008. 1000 Genomes project. *Nat Biotechnol* **26:** 256.

Takai D, Jones PA. 2002. Comprehensive analysis of CpG islands in human chromosomes 21 and 22. *Proc Natl Acad Sci U S A* **99:** 3740-3745.

Teaktong T, Graham A, Court J, Perry R, Jaros E, Johnson M, Hall R, Perry E. 2003. Alzheimer's disease is associated with a selective increase in alpha7 nicotinic acetylcholine receptor immunoreactivity in astrocytes. *Glia* **41:** 207-211.

Teschendorff AE, Menon U, Gentry-Maharaj A, Ramus SJ, Weisenberger DJ, Shen H, Campan M, Noushmehr H, Bell CG, Maxwell AP et al. 2010. Age-dependent DNA methylation of genes that are suppressed in stem cells is a hallmark of cancer. *Genome Res* **20:** 440-446.

Tjabringa G, Bergers M, van Rens D, de Boer R, Lamme E, Schalkwijk J. 2008. Development and validation of human psoriatic skin equivalents. *Am J Pathol* **173**: 815-823.

2010. Time for the epigenome. *Nature* **463:** 587.

Urdinguio RG, Sanchez-Mut JV, Esteller M. 2009. Epigenetic mechanisms in neurological diseases: genes, syndromes, and therapies. *Lancet Neurol* **8:** 1056-1072.

Vaughn MW, Tanurdzic M, Lippman Z, Jiang H, Carrasquillo R, Rabinowicz PD, Dedhia N, McCombie WR, Agier N, Bulski A et al. 2007. Epigenetic natural variation in Arabidopsis thaliana. *PLoS Biol* **5:** e174.

Weber M, Davies JJ, Wittig D, Oakeley EJ, Haase M, Lam WL, Schubeler D. 2005. Chromosome-wide and promoter-specific analyses identify sites of differential DNA methylation in normal and transformed human cells. *Nat Genet* **37:** 853-862.

Weber M, Hellmann I, Stadler MB, Ramos L, Paabo S, Rebhan M, Schubeler D. 2007. Distribution, silencing potential and evolutionary impact of promoter DNA methylation in the human genome. *Nat Genet* **39:** 457-466.

Widschwendter M, Fiegl H, Egle D, Mueller-Holzner E, Spizzo G, Marth C, Weisenberger DJ, Campan M, Young J, Jacobs I et al. 2007. Epigenetic stem cell signature in cancer. *Nat Genet* **39:** 157-158.

Zhang X, Yazaki J, Sundaresan A, Cokus S, Chan SW, Chen H, Henderson IR, Shinn P, Pellegrini M, Jacobsen SE et al. 2006. Genome-wide high-resolution mapping and functional analysis of DNA methylation in arabidopsis. *Cell* **126:** 1189-1201.

Zhang Y, Rohde C, Tierling S, Jurkowski TP, Bock C, Santacruz D, Ragozin S, Reinhardt R, Groth M, Walter J et al. 2009. DNA methylation analysis of chromosome 21 gene promoters at single base pair and single allele resolution. *PLoS Genet* **5:** e1000438.

Zilberman D, Gehring M, Tran RK, Ballinger T, Henikoff S. 2007. Genome-wide analysis of Arabidopsis thaliana DNA methylation uncovers an interdependence between methylation and transcription. *Nat Genet* **39:** 61-69.

Acknowledgements

This work was supported by European Grants CANCERDIP HEALTH-F2-2007-200620, LSHG-CT-2006-018739–ESTOOLS, LSHC-CT-2006-037297–MCSCs, the Dr. Josef Steiner Cancer Research Foundation Award, the Fondo de Investigaciones Sanitarias Grant PI08-1345, Consolider Grant MEC09-05, the Spanish Association Against Cancer (AECC), Spanish Ministry of Education and Science (SAF2009-07319), the Lilly Foundation Biomedical Research Award, Fundacio Cellex and the Health Department of the Catalan Government (Generalitat de Catalunya). R.S. is supported by BMBF and Deutsche Krebshilfe. J.B. is supported in part by the University College London Cancer Institute Experimental Cancer Medicine Centre and the University College London Hospitals and University College London Comprehensive Biomedical Research Centre. M.E. is an Institucio Catalana de Recerca i Estudis Avançats (ICREA) Research Professor.

Author Contributions

A.F.F., Y.A., C.B. and M.E. conceived and designed the experiments. All authors analyzed the data. A.F.F., Y.A., C.B. and M.E. wrote the manuscript.

Figure Legends

Figure 1. DNA methylation fingerprints for human normal tissues. A. Unsupervised hierarchical clustering and heatmap including CpG dinucleotides with differential DNA methylation encountered between different normal primary samples. Tissue type and development layers are displayed in different colors indicated in the figure legends. Average methylation values are displayed from 0 (green) to 1 (red) **B.** Deviation plot for the 1,322 CpG sites studied in leukocyte samples showing that little CpG methylation heterogeneity (yellow area) occurs overall at CpG sites within CpG islands (red lines in the track below), while more differences in CpG methylation are observed outside CpG islands (blue lines in the track below). **C.** Unsupervised hierarchical clustering and heatmap including sets of genes with high correlation values between hypomethylation (up) and hypermethylation (down) with aging. **D.** Unsupervised hierarchical clustering and heatmap showing the DNA methylation patterns of embryonic and adult stem cells, comparing them with corresponding normal and differentiated tissues (muscle, bone and neuron; and muscle and brain, respectively).

Figure 2. DNA methylation fingerprint of human cancer. A. Unsupervised hierarchical clustering and heatmap showing distinction of primary tumor DNA methylation fingerprints according to the tissue of origin. **B.** Unsupervised hierarchical clustering and heatmap of primary tumors excluding CpG sites with tissue-specific methylation. **C.** Above**,** Pie charts displaying the percentage of hypermethylated CpG sites (red) and hypomethylated CpG sites (green) in human malignancies, and their distribution in CpG islands (CGI in red) and outside CpG islands (non-CGI in blue). Below, Deviation plot for the 1,322 CpG sites showing the great methylation heterogeneity (yellow area) of primary tumors in comparison with normal primary tissues.

Figure 3. Scenarios of DNA methylation changes in human tumorigenesis. A. Bart plot showing the CpG hypermethylation or hypomethylation changes observed when comparing paired normal–tumor tissues from the same

colorectal cancer patient. They can be distinguished if the methylation change occurs in CpG island (CGI) or non-CpG island (non CGI) associated CpG. **B.** Unsupervised hierarchical clustering and heatmap including a set of specific CpG sites that undergo differential DNA methylation only in cancer cell lines. **C.** Deviation plot for the 1,322 CpG sites shows greater CpG methylation heterogeneity (yellow area) in established tumors (colon, breast and endometrial cancers) than in their corresponding premalignant lesions. **D.** DNA methylation unsupervised clustering analyses and heatmap of primary tumors, local liver metastases and distant brain metastases from the same colorectal cancer patient. A CpG methylation-specific pattern for brain metastases (green lanes) is observed. **E.** CpG methylation prediction heatmap showing the CUP classification to a specific tumor type.

Figure 4. DNA methylation fingerprint in non-tumoral human diseases. A. Unsupervised hierarchical clustering and heatmap of several non-tumoral diseases showing distinct DNA methylation profiles. **B.** Unsupervised hierarchical clustering and heatmap showing significant differences between the DNA methylation patterns of dementia with Lewy bodies and normal controls. The CpG methylation platform used was unable to detect significant differences in the case of Alzheimer's vs. healthy brain tissues. **C.** Unsupervised hierarchical clustering and heatmap showing differences between dementia with Lewy bodies and neuroectodermal tumors (glioma and neuroblastoma).

Figure 5. A DNA methylation fingerprint of 1,628 human samples. Unsupervised hierarchical clustering and heatmap of all the CpG methylation maps obtained in the study, by tissue and disease type.

Figure 1

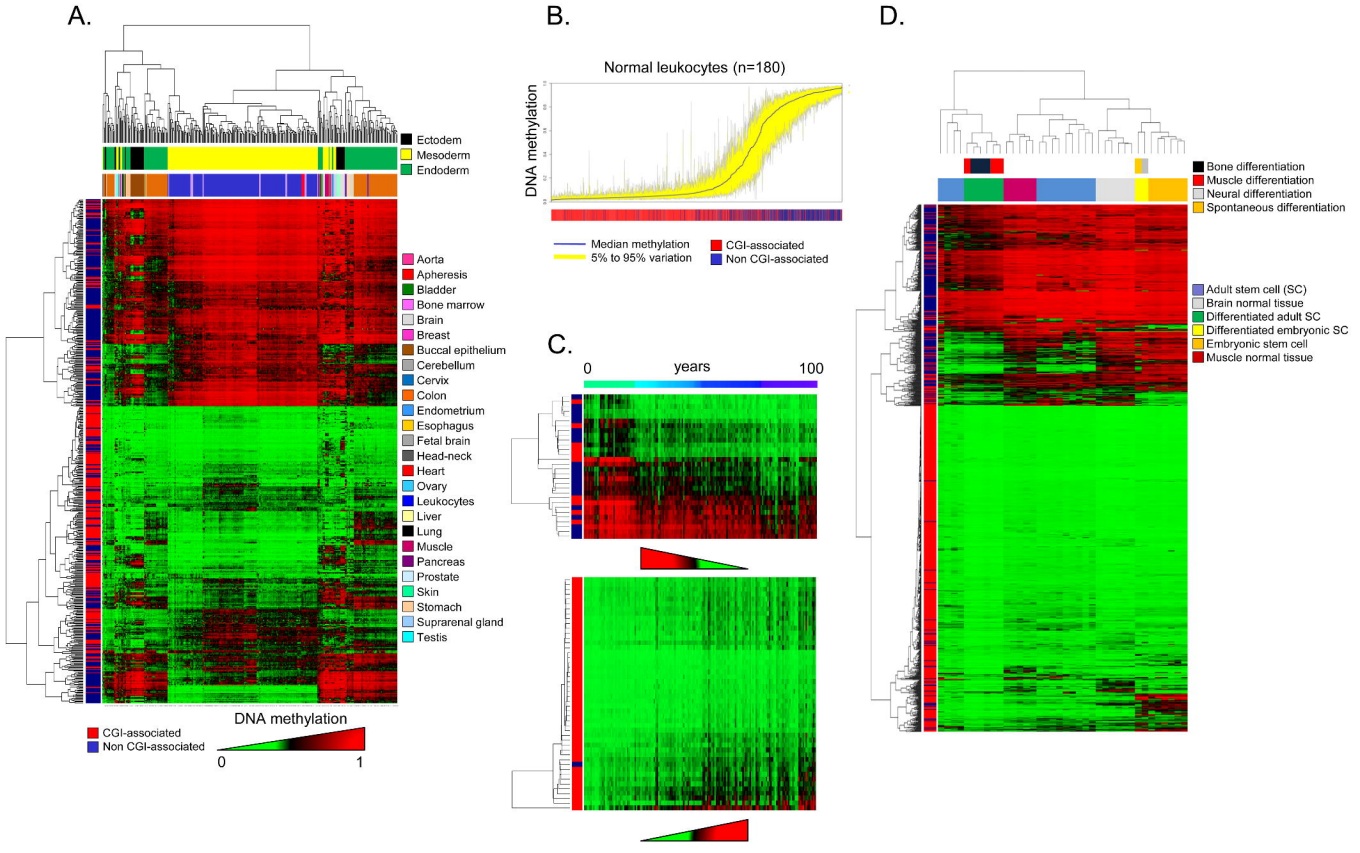
A.
Ectoderm
Mesoderm
Endoderm
Aorta
Apheresis
Bladder
Bone marrow
Brain
Breast
Buccal epithelium
Cerebellum
Cervix
Colon
Endometrium
Esophagus
Fetal brain
Head-neck
Heart
Ovary
Leukocytes
Liver
Lung
Muscle
Pancreas
Prostate
Skin
Stomach
Suprarenal gland
Testis
DNA methylation
CGI-associated
Non CGI-associated
0
1
B.
Normal leukocytes (n=180)
DNA methylation
Median methylation
5% to 95% variation
CGI-associated
Non CGI-associated
C.
0
years
100
D.
Bone differentiation
Muscle differentiation
Neural differentiation
Spontaneous differentiation
Adult stem cell (SC)
Brain normal tissue
Differentiated adult SC
Differentiated embryonic SC
Embryonic stem cell
Muscle normal tissue

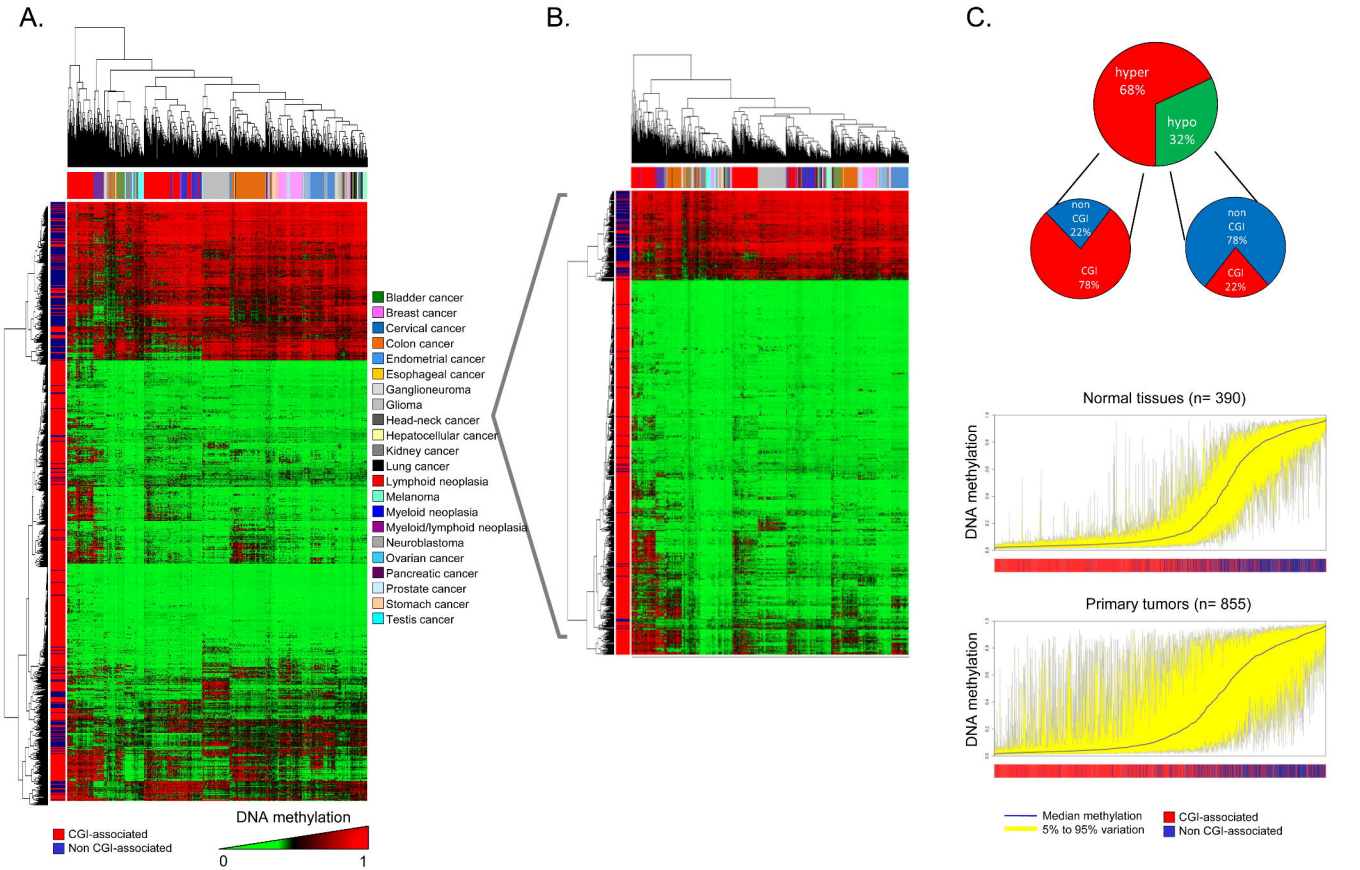
A.
B.
C.
Bladder cancer
Breast cancer
Cervical cancer
Colon cancer
Endometrial cancer
Esophageal cancer
Ganglioneuroma
Glioma
Head-neck cancer
Hepatocellular cancer
Kidney cancer
Lung cancer
Lymphoid neoplasia
Melanoma
Myeloid neoplasia
Myeloid/lymphoid neoplasia
Neuroblastoma
Ovarian cancer
Pancreatic cancer
Prostate cancer
Stomach cancer
Testis cancer
CGI-associated
Non CGI-associated
DNA methylation
0
1
hyper 68%
hypo 32%
non CGI 22%
CGI 78%
non CGI 78%
CGI 22%
Normal tissues (n= 390)
Primary tumors (n= 855)
DNA methylation
Median methylation
5% to 95% variation
CGI-associated
Non CGI-associated

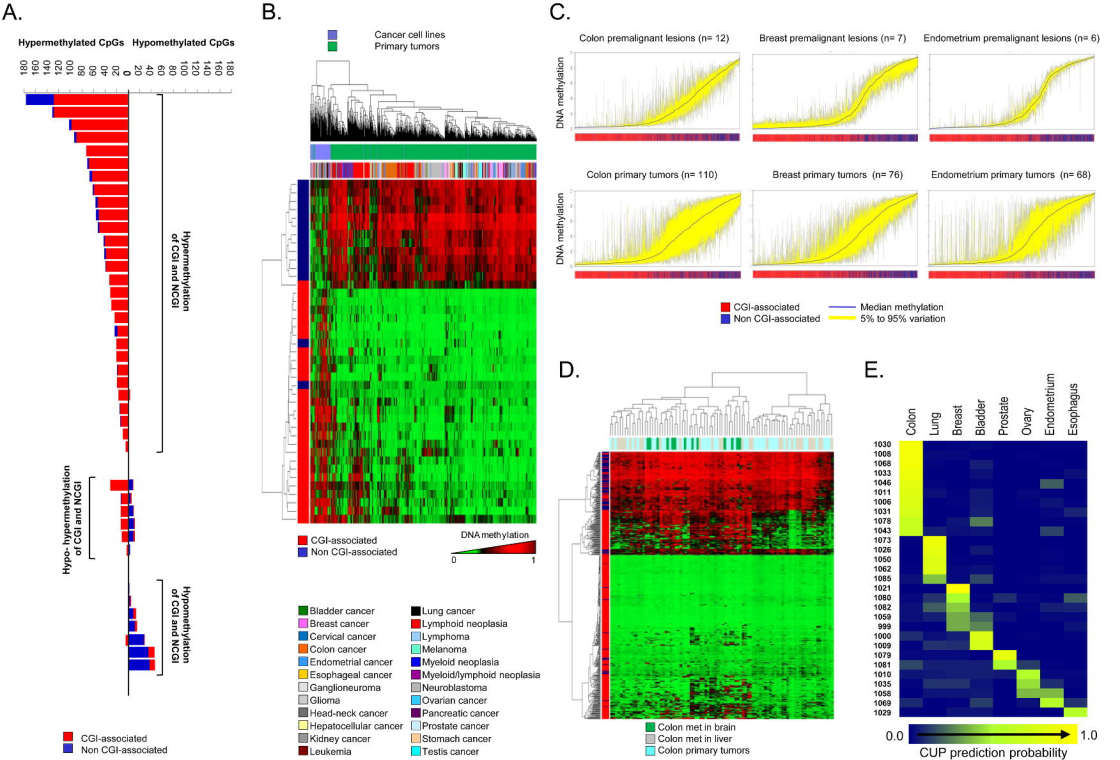
A.
Hypermethylated CpGs
Hypomethylated CpGs
Hypermethylation of CGI and NCGI
Hypo- hypermethylation of CGI and NCGI
Hypomethylation of CGI and NCGI
CGI-associated
Non CGI-associated
B.
Cancer cell lines
Primary tumors
CGI-associated
Non CGI-associated
DNA methylation
Bladder cancer
Breast cancer
Cervical cancer
Colon cancer
Endometrial cancer
Esophageal cancer
Ganglioneuroma
Glioma
Head-neck cancer
Hepatocellular cancer
Kidney cancer
Leukemia
Lung cancer
Lymphoid neoplasia
Lymphoma
Melanoma
Myeloid neoplasia
Myeloid/lymphoid neoplasia
Neuroblastoma
Ovarian cancer
Pancreatic cancer
Prostate cancer
Stomach cancer
Testis cancer
C.
Colon premalignant lesions (n= 12)
Breast premalignant lesions (n= 7)
Endometrium premalignant lesions (n= 6)
Colon primary tumors (n= 110)
Breast primary tumors (n= 76)
Endometrium primary tumors (n= 68)
DNA methylation
CGI-associated
Non CGI-associated
Median methylation
5% to 95% variation
D.
Colon met in brain
Colon met in liver
Colon primary tumors
E.
Colon
Lung
Breast
Bladder
Prostate
Ovary
Endometrium
Esophagus
0.0
1.0
CUP prediction probability

Figure 4

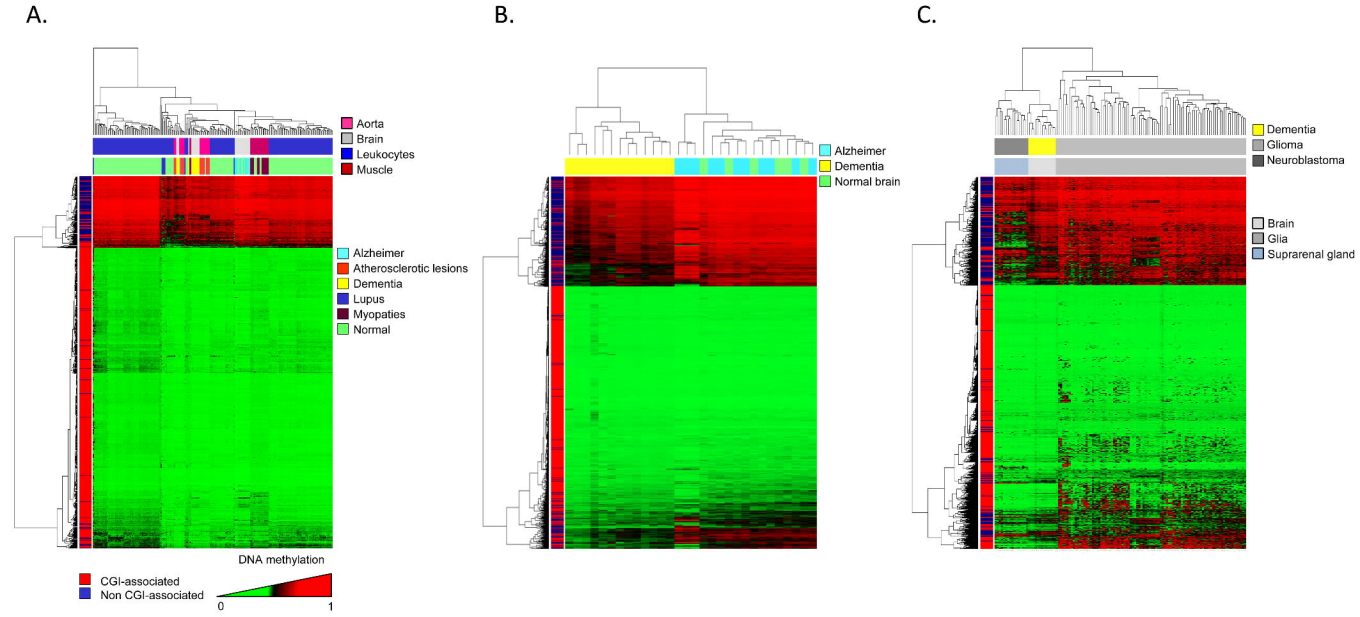
A.
Aorta
Brain
Leukocytes
Muscle
Alzheimer
Atherosclerotic lesions
Dementia
Lupus
Myopaties
Normal
DNA methylation
CGI-associated
Non CGI-associated
0
1
B.
Alzheimer
Dementia
Normal brain
C.
Dementia
Glioma
Neuroblastoma
Brain
Glia
Suprarenal gland

Figure 5

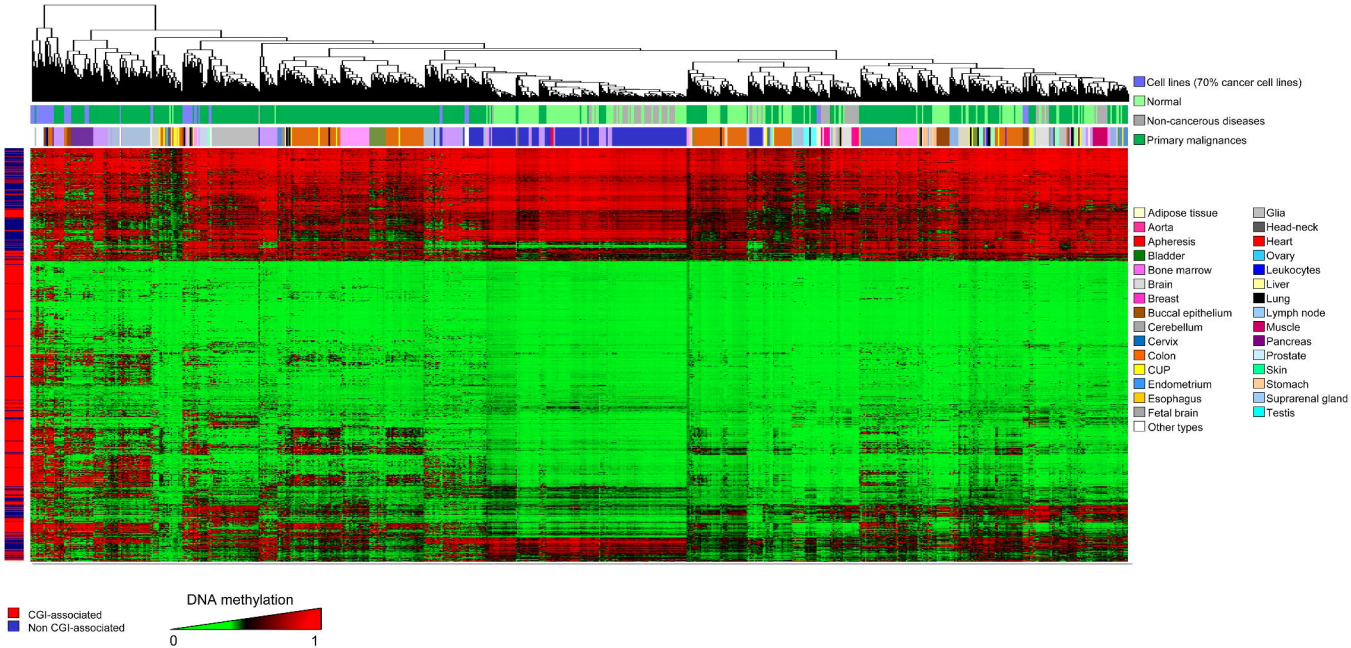
Cell lines (70% cancer cell lines)
Normal
Non-cancerous diseases
Primary malignances
Adipose tissue
Aorta
Apheresis
Bladder
Bone marrow
Brain
Breast
Buccal epithelium
Cerebellum
Cervix
Colon
CUP
Endometrium
Esophagus
Fetal brain
Other types
Glia
Head-neck
Heart
Ovary
Leukocytes
Liver
Lung
Lymph node
Muscle
Pancreas
Prostate
Skin
Stomach
Suprarenal gland
Testis
CGI-associated
Non CGI-associated
DNA methylation
0
1